High-Strength Copper/Silver Alloys Processed by Cold Spraying for DC and Pulsed High Magnetic Fields

Simon Tardieu, Hanane Idrir, Christophe Verdy, Olivier Jay, Nelson Ferreira, François Debray, Anne Joulain, Christophe Tromas, Ludovic Thilly, Florence Lecouturier-Dupouy

magnetochemistry

MDPI

Article

High-Strength Copper/Silver Alloys Processed by Cold Spraying for DC and Pulsed High Magnetic Fields

Simon Tardieu [1,2,*], Hanane Idrir [3], Christophe Verdy [4], Olivier Jay [1,2], Nelson Ferreira [1,2], François Debray [1,2], Anne Joulain [3], Christophe Tromas [3], Ludovic Thilly [3] and Florence Lecouturier-Dupouy [1,2]

1 CNRS, Laboratoire National des Champs Magnétiques Intenses, INSA-UGA-UPS-EMFL, 38000 Grenoble, France; olivier.jay@lncmi.cnrs.fr (O.J.); nelson.ferreira@lncmi.cnrs.fr (N.F.); francois.debray@lncmi.cnrs.fr (F.D.); florence.lecouturier@lncmi.cnrs.fr (F.L.-D.)
2 CNRS, Laboratoire National des Champs Magnétiques Intenses, INSA-UGA-UPS-EMFL, 31400 Toulouse, France
3 Institut Pprime, UPR 3346 CNRS-Université de Poitiers-ENSMA, Boulevard M. et P. Curie, TSA 41123, 86073 Poitiers Cedex 9, France; hanane.idrir@univ-poitiers.fr (H.I.); anne.joulain@univ-poitiers.fr (A.J.); christophe.tromas@univ-poitiers.fr (C.T.); ludovic.thilly@univ-poitiers.fr (L.T.)
4 ICB, UMR 6303, CNRS, Université Bourgogne Franche-Comté, UTBM, 90010 Belfort, France; christophe.verdy@utbm.fr
* Correspondence: simon.tardieu@lncmi.cnrs.fr; Tel.: +33-(0)5-6217-2979

Abstract: High-strength, high-conductivity copper/silver-alloyed materials were prepared by cold-spray (CS) manufacturing. For DC high-field application at room temperature, bulk Cu/Ag (5% vol. Ag) alloys with high mechanical properties and high electrical conductivity can be obtained by CS and post-heat treatments. For pulsed-field application at liquid nitrogen temperature, bulk Cu/Ag (5% vol. Ag) alloys serve as precursors for room-temperature wire drawing. The Cu/Ag-alloyed bulk CS deposit presents a high yield strength of about 510 MPa with a corresponding electrical resistivity of 1.92 μΩ·cm (at 293 K). The Cu/Ag-alloyed wires show a very high ultimate tensile strength (1660 MPa at 77 K or 1370 MPa at 293 K) and low electrical resistivity (1.05 μΩ·cm at 77 K or 2.56 μΩ·cm at 293 K). Microstructural studies via STEM allow us to understand this very high level of mechanical strength. The results evidence that materials developed by CS exhibit very high mechanical properties compared to materials prepared by other routes, due to the high velocity of the deposited particles, which leads to high initial deformation rates and specific microstructural features.

Keywords: alloy; cold spray; copper; magnetic field; silver; wire drawing

Citation: Tardieu, S.; Idrir, H.; Verdy, C.; Jay, O.; Ferreira, N.; Debray, F.; Joulain, A.; Tromas, C.; Thilly, L.; Lecouturier-Dupouy, F. High-Strength Copper/Silver Alloys Processed by Cold Spraying for DC and Pulsed High Magnetic Fields. *Magnetochemistry* **2024**, *10*, 15. https://doi.org/10.3390/magnetochemistry10030015

Academic Editor: Joan-Josep Suñol

Received: 29 January 2024
Revised: 15 February 2024
Accepted: 16 February 2024
Published: 21 February 2024

1. Introduction

Located across two sites, the Laboratoire National des Champs Magnétiques Intenses (LNCMI) aims to offer static magnetic fields up to 43 T [1] at its Grenoble (France) site and non-destructive pulsed magnetic fields up to 100 T [2] at its Toulouse (France) site to internal and external researchers. In both cases, to provide the magnetic fields, a high electrical current must be injected into an appropriate resistive coil. Conductor materials must exhibit a very high mechanical strength in order to withstand the stresses caused by the Lorentz forces induced by the generation of the magnetic field. Moreover, conductors that make up the resistive magnets must have an electrical resistivity as low as possible. In order to limit the heating due to the Joule effect, conductors are continuously cooled by water (for static magnetic fields) or immersed in liquid nitrogen (for non-destructive pulsed magnetic fields). Thus, high-field polyhelix DC magnets and multi-turn pulsed magnets require, respectively, bulk materials and wires combining high mechanical strength and high electrical conductivity.

For several decades, Cu/Ag-alloyed wires (6–24% wt. Ag) have been prepared by classical metallurgical routes involving high temperatures (melting, solidification) and

drawing [3–6]. They exhibit a high ultimate tensile strength (UTS) of 965 MPa at 293 K and 1160 MPa at 77 K, but too high electrical resistivity (2.4 μΩ·cm at 293 K and 0.81 μΩ·cm at 77 K) due to their eutectic microstructure and high silver content.

In the last decade, it has been demonstrated that the use of powder metallurgy combined with a low silver content while tailoring micro/nanostructuring allows the production of conductors combining high mechanical strength and high electrical conductivity [7–12].

In this work, the cold-spray (CS) processing technique is used to produce alloyed bulk Cu/Ag (5% vol. Ag) material. Using this CS technique, a fluidized powder feedstock is fed into a nozzle at a high pressure so that the powder particles are accelerated within the gas stream to reach very high velocities (1200 m/s) [13]. The bounding during impact depends on the capacity of the projected powder to be plastically deformed; it is thus necessary that the powder exceeds a critical speed at the moment of impact with the substrate [14–16]. At the highly deformed interface of the powder/substrate, an adiabatic shear instability [17,18] generates a rapid local temperature rise and confines (at the interface) melting phenomena [19], and grains are refined through dynamic recrystallization [20,21].

By the CS technique, it is expected that the bulk Cu/Ag alloys obtained present high mechanical strength due to the high deformation of powders upon impact and the resulting peculiar microstructure and low resistivity due to the low silver content. In addition, the drawing ability of CS-alloyed Cu/Ag precursors is investigated in order to enhance the strength of wires for multi-turn pulsed magnets.

2. Experimental Procedure

2.1. Powder Preparation

The raw material for the Cu/Ag-alloyed powder production was Cu-c2 bars and high-purity silver granulates (99.99% purity). The feedstock Cu/Ag-alloyed powder was obtained by high-pressure gas atomization with argon. The process is described in more detail in previous work [9]. The so-obtained Cu/Ag-alloyed powder shows a Ag content of 5.35 weight % (4.60 vol. % Ag). Samples are designated Cu/5Ag hereafter. The particle size is between 10 μm and 50 μm.

2.2. Cold-Spray Deposition

The CS system used is equipped with a closed-loop circulating device in order to perform the deposition under a helium atmosphere, and is described in previous work [7]. The helium atmosphere avoids oxygen contamination during the deposition process and allows us to reach high particle velocity (>700 m/s) [8]. The Cu/5Ag-alloyed powder was sprayed on a rotating cylindrical substrate using a vertically moving CS gun. Each vertical passage of the CS gun allows the deposition of a layer of approximately 150 μm with a flow rate of 106 g/min. The final dimensions of the Cu/5Ag bulk deposit were as follows: 192 mm in height, 50 mm internal diameter, and 160 mm external diameter (Figure 1).

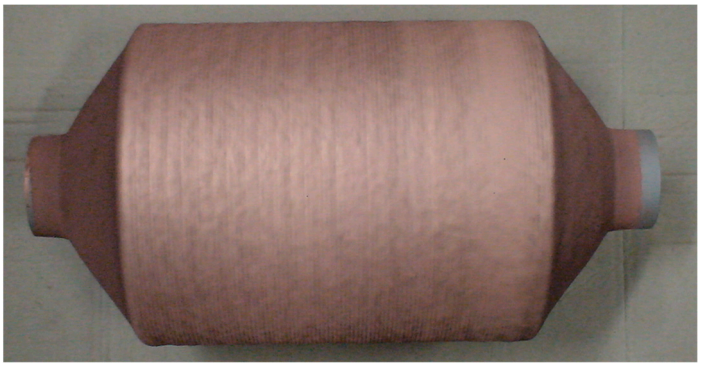

Figure 1. Photograph of the Cu/5Ag CS deposit.

2.3. Wire Preparation

A cylinder of 7 mm in diameter and 50 mm in length serving as starting material for wire drawing was collected by spark erosion applied in the longitudinal direction of the CS deposit. Thus, the successive layers were parallel to the wire-drawing direction. The cylinder was wire-drawn at room temperature through conical WC dies in about 40 passes to obtain wires with decreasing diameters down to 0.2 mm (without breaking). Samples of wires were 400 mm long. During wire preparation no heat treatment was carried out.

2.4. Characterization

2.4.1. Microstructure

The particle observation was carried out by scanning electron microscopy (SEM) with a JEOL JSM 7800 F device (JEOL Europe SAS., 78290 Croissy-sur-Seine, France). The particle size distribution was determined by laser light scattering using a Malver Mastersizer particle size analyzer.

The microstructure of CS samples was characterized by transmission electron microscopy (TEM) using a Thermofisher Scientific Talos F200S G2 (Thermo Fisher Scientific Inc., Waltham, MA, USA) equipped with a double tilt and operated at an acceleration voltage of 200 kV. TEM thin foils were extracted by a Focused Ion Beam (FIB, Helios NanoLab DualBeam G3 CX, ThermoFisher, Thermo Fisher Scientific Inc., Waltham, MA, USA) via the lift-out technique. The thin foils were cut perpendicular or parallel to the drawing direction, with the following typical dimensions: about 15 μm in length, 10 μm in height, and less than 70 nm in thickness (after several FIB thinning steps at a reduced current).

2.4.2. Macroscopic Properties of Cu/5Ag Bulk Material

To characterize the mechanical and electrical properties of the bulk material, the samples were machined by wire cutting in the deposited cylinder. For both mechanical and electrical characterizations, some of the samples were kept in the as-deposited condition, while others were subjected to different thermal treatments. The heat treatments were carried out in an electrical furnace under vacuum for 8 h and at several temperatures—320 °C, 330 °C and 340 °C—followed by cooling under vacuum.

Tensile tests were performed up to fracture at room temperature using an MTS DY35 machine equipped with a 20 kN force gauge with a constant ram speed of 0.25 mm·min^{-1}. Resistivity measurements were performed using a four-terminal sensing device with 100 mA for input current. A thermostated bath, Lauda Alpha type A (Lauda, 97922 Lauda-Königshofen, Germany), filled with di-ionized water was used in order to maintain the samples at 20 ± 1 °C.

2.4.3. Macroscopic Properties of Cu/5Ag Wires

The density of the samples was measured by Archimedes' method. Tensile tests on wires were performed (INSTRON 1195 machine, Instron, High Wycombe, Buckinghamshire, UK) at room temperature (293 K) and at liquid nitrogen temperature (77 K) on 200 mm long wires. Applied stresses were measured by appropriated force gauges (1000 N or 250 N) at a speed of 1 mm·min^{-1} (strain rate = 10^{-3} s^{-1}). Vickers microhardness was determined from indentation tests (Shimadzu HMV M3; loading = 1 N, 10 s, room temperature) on flat surfaces obtained by polishing. The reported Vickers microhardness values are the average of 5 tests or more. The distance between two successive indentations was 10 times the diagonal length of the indent.

The electrical resistivity of 400 mm long wires was measured at 293 K and 77 K using the four-probe method with a maximum current of 100 mA to avoid heating the wires.

3. Results and Discussion

3.1. Microstructure

The Cu/5Ag-alloyed powder presented spherical particles with few satellites (Figure 2) and a unimodal particle size distribution (d_{10} = 12 μm, d_{50} = 20 μm, and d_{90} = 37 μm).

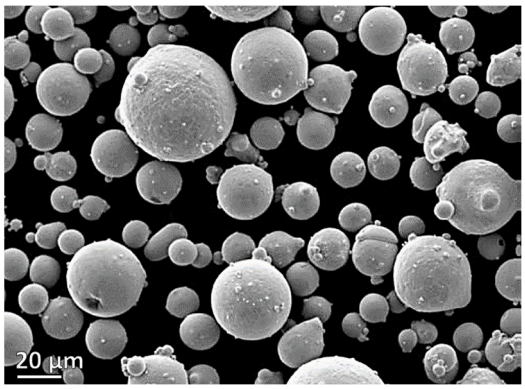

Figure 2. SEM image of the Cu/5Ag powder particles.

The CS deposit was 98.3% ± 1.0% dense (measured by Archimedes' method). The microstructure of the CS deposit was investigated by optical microscopy, SEM, and TEM. The optical microscopy image of the CS deposit shows some macroscopic (>10 µm) Ag-rich domains and porosities (see circles in Figure 3). The energy-dispersive X-ray spectroscopy (EDS) analysis (Figure 4) confirms the initial silver content and shows that the Ag content in localized Ag-dense areas would be about 60 vol. %.

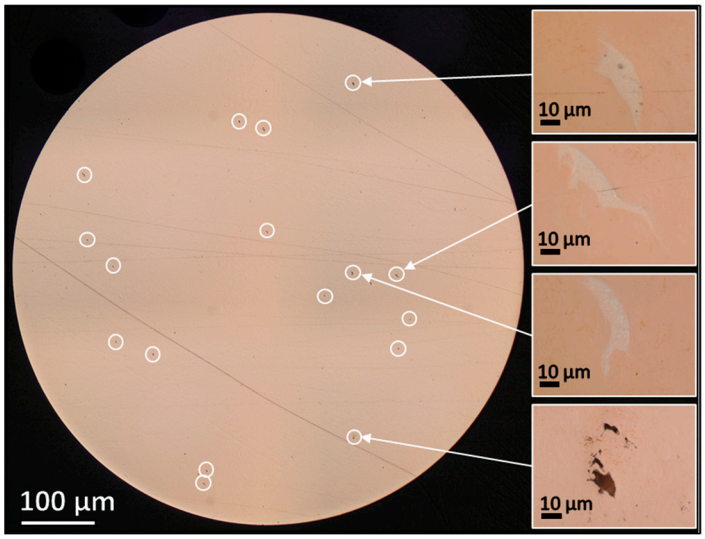

Figure 3. Optical microscopy image of the CS deposit 7 mm diameter cylinder serving as starting material for wire drawing. White circles indicate Ag-rich domains and macroscopic porosities.

Figure 5a presents a general view of the microstructure of the CS deposit, observed in HAADF STEM mode. One can observe that, as expected, the microstructure is very distorted as a direct result of the CS technique. On STEM-EDS elemental maps (Figure 5b,c), it is possible to observe that Ag is present in the entire sample, indicating that the CS deposit is mainly composed of Cu-rich solid solution. Some areas appear richer in silver: this confirms the presence of Ag-rich solid solution in specific regions, as already observed at the macroscopic scale (Figure 3).

Fine wires are prepared by wire-drawing the cylinders extracted from the bulk CS deposit at room temperature. The wires with a diameter of 4 mm have a density of 98.8 ± 1.0%. The density is probably higher for finer wires, but the uncertainty is too high to give meaningful values.

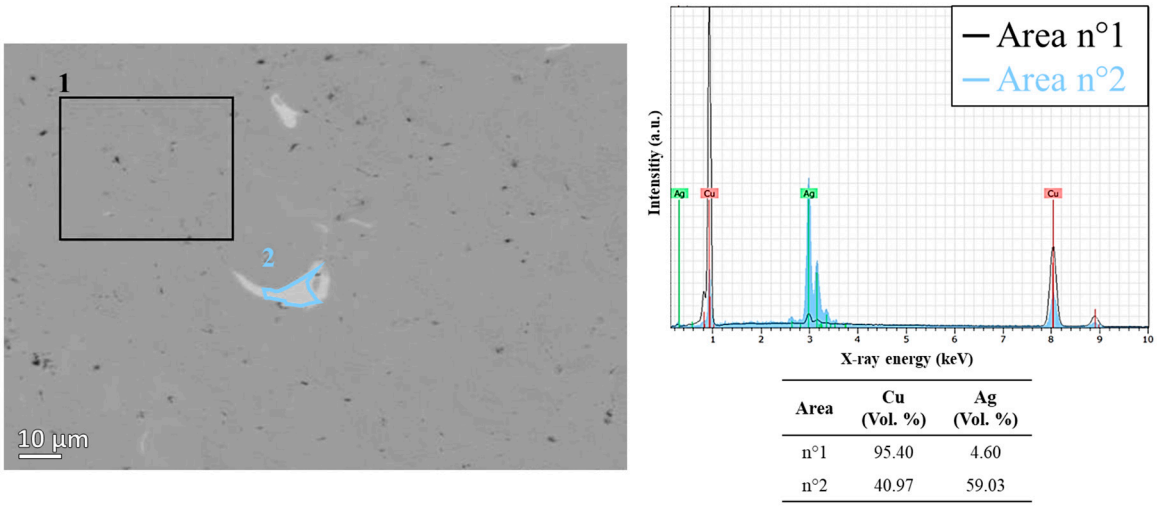

Area	Cu (Vol. %)	Ag (Vol. %)
n°1	95.40	4.60
n°2	40.97	59.03

Figure 4. SEM image and corresponding EDS spectra of the CS deposit. The black (1) and blue (2) areas indicate the EDS analysis areas.

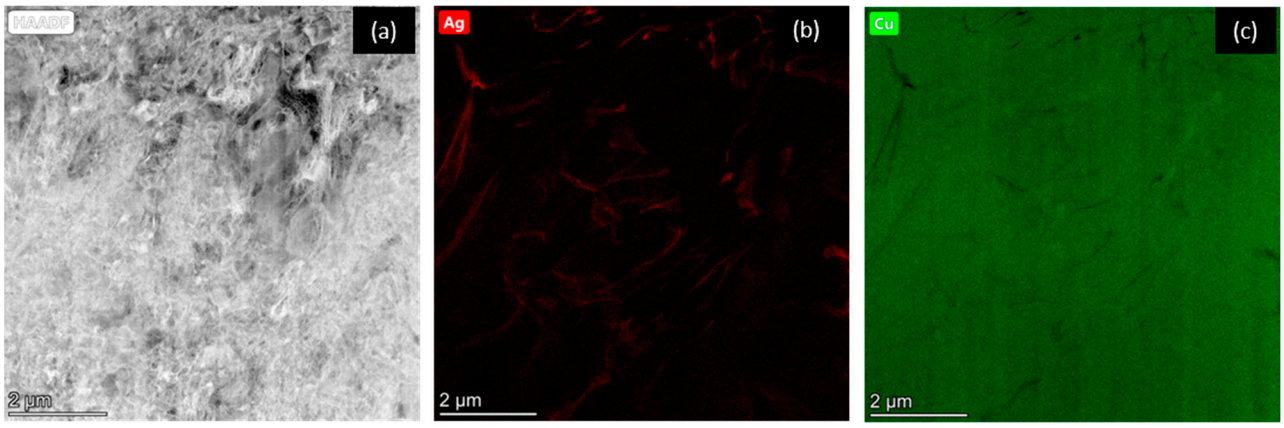

Figure 5. STEM HAADF image (**a**) and STEM-EDS elemental mappings (**b**,**c**) of the CS deposit.

The microstructures of the transversal section (Figure 6) and longitudinal section (Figure 7) of the wire with a diameter of 0.5 mm were investigated by TEM. The cross-section of the wire revealed a reduction in grain size following cold drawing, as well as a microstructure with two distinct features: regions with elongated ribbon-like grains (black rectangle, Figure 6a), and regions with nearly equiaxed grains (yellow arrows). This microstructure is believed to be representative of the CS deposition process. Indeed, the formation of elongated grains may happen at particle/particle interfaces as a result of the significant plastic deformation experienced by the projected particles during deposition [22]. The particle interiors are less impacted and keep their equiaxed structure. This dual microstructure obviously persists after deformation, despite a reduction in grain size. As observed in the CS deposit, the fine wire is predominantly composed of a Cu-rich solid solution and some Ag-rich solid solution domains, as presented in Figure 6b,c.

The refinement of the microstructure observed on the cross-section of the wire is accompanied by a strong elongation of the grains in the longitudinal direction (i.e., the drawing axis), as presented in Figure 7. The grains are elongated along the thin foil (Figure 7a,b, at different scales), and their length can reach several tens of micrometers (the exact length is usually larger than the thin foil length, so potentially longer than 25 µm). Some grains exhibit twins (see arrows in Figure 7b).

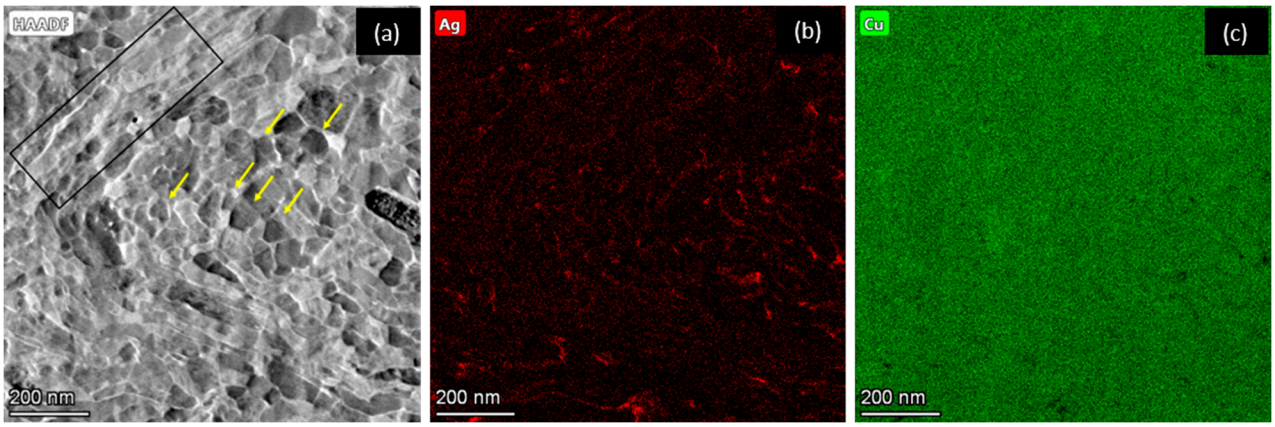

Figure 6. STEM HAADF image (**a**) and STEM-EDS Ag mapping (**b**) and Cu mapping (**c**) of the transversal section of wire (Ø = 0.5 mm). The yellow arrows indicate regions with nearly equiaxed grains and the black rectangle indicates regions with elongated ribbon-like grains.

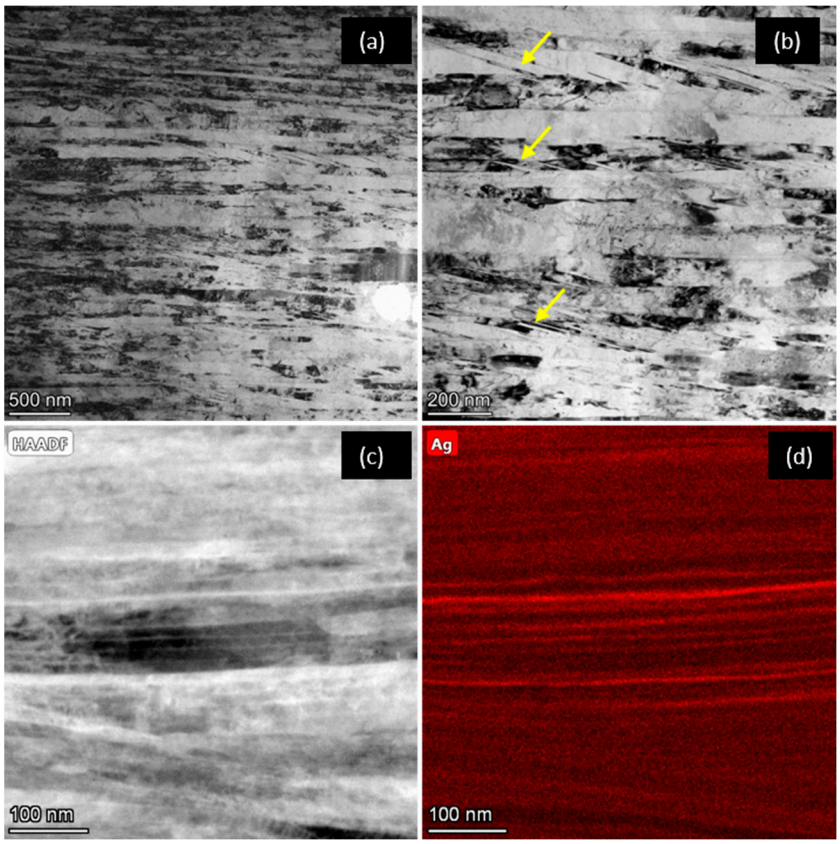

Figure 7. TEM images (**a**,**b**), STEM HAADF image (**c**), and STEM-EDS Ag mapping (**d**) of the longitudinal section of wire (Ø = 0.5 mm). The yellow arrows indicate twins.

As mentioned earlier, the sample is predominantly composed of a copper-rich solid solution, with the presence of certain areas containing a Ag-rich solid solution. These areas can be interpreted as regions where silver diffused during the CS deposition, and/or during the initial stages of wire drawing. Subjected to the drawing process, these regions were deformed to form silver-rich elongated structures extending over several micrometers (Figure 7c,d).

3.2. Mechanical Properties and Electrical Resistivity

3.2.1. Bulk Material

For the production of a steady magnetic field, polyhelix technology is used. It consists of the assembly of a set of cylinders cut helicoidally by sparking erosion technique to form the coils. A typical high-field magnet necessitates cylinders with diameters up to 380 mm with various thicknesses from 5 to 20 mm, or even 100 mm when using the radially cooled technique (Figure 8).

Figure 8. Helices (tubes cut helicoidally) for steady-field production. The outer diameter of the largest tube (right) is 372 mm. The weight of the powder necessary for the corresponding deposit before final machining is 120 kg. Today, all tubes are prepared using the CS bulk deposit process.

When using forged products for a given alloy, the specifications degrade with increasing diameter due to the technical limitation of the mechanical hardening of large-size pieces. This is no longer the case for CS deposits where the properties are independent of the deposit diameter. Nevertheless, the CS technology is intrinsically anisotropic. Therefore, the anisotropy of bulk cylinders is qualified thanks to the extraction of tensile test pieces in the three directions of a test cylinder: radial (direction of the spray), longitudinal (the direction used for the precursors for wire drawing) and tangential (corresponding to the surface rotation during the processing). The results of the tensile tests and the conductivity measurements performed on the as-deposited and heat-treated samples are shown in Figure 9a,b, respectively.

Firstly, regarding the yield strength, by looking only at the result for the as-deposited material, one can see that the yield strength for the radial direction is under 500 MPa, while it is around 630 MPa for the tangential and longitudinal directions. This is due to the way that the cylinder is manufactured by the CS process: the CS gun deposits the material layer by layer in the radial direction. Further investigations have shown the formation of cracks along the interface of these layers which result in the fracture of the sample [9]. However, by applying a heat treatment to the material, the yield strength of the material is the same in the three directions with the following mean values: 560 MPa with an 8 h heat treatment at 320 °C, 530 MPa with an 8 h heat treatment at 330 °C, and 490 MPa with an 8 h heat treatment at 340 °C. This improvement in the isotropy of the material may be explained by the enhancement in metallurgical bonding between particles at the layers' interfaces associated with the thermal treatment [23,24].

Secondly, taking into account the impact of the thermal treatments on conductivity, other microstructural changes occur like recovery, recrystallization, and grain growth. However, conductivity does not show a clear evolution with the increase in temperature of the thermal treatment, in contrast to yield strength which shows a gradual decrease. Thus, the changes may be mostly related to recovery and recrystallization.

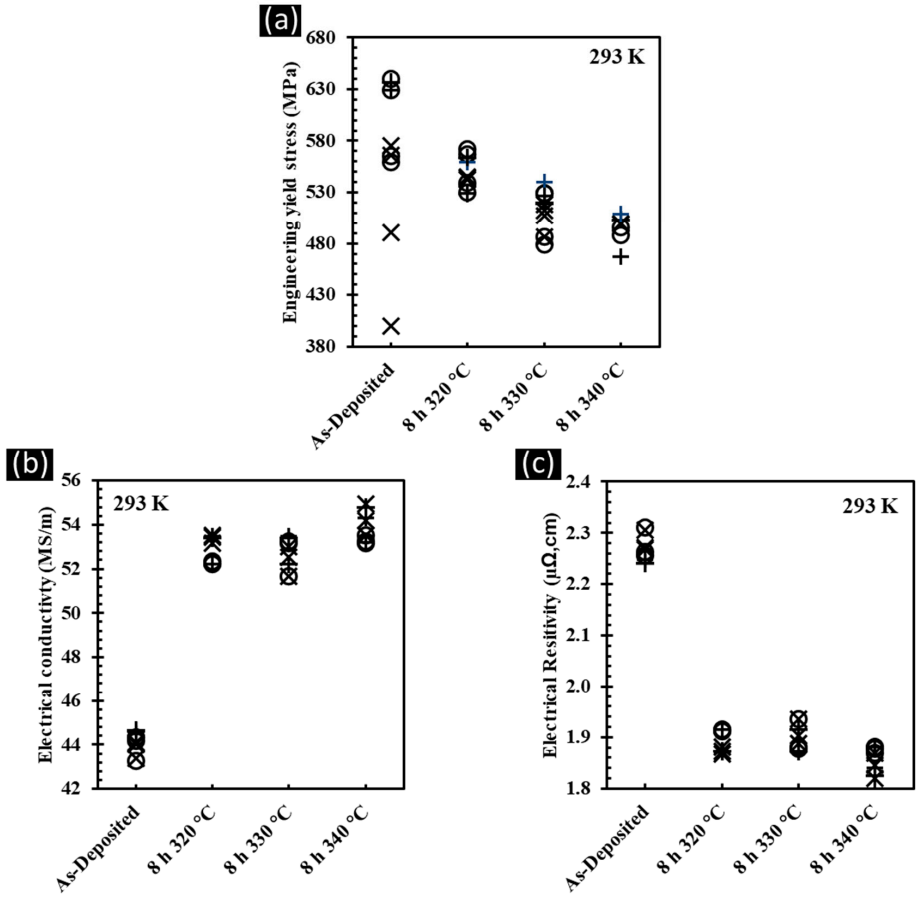

Figure 9. (**a**) Engineering yield strength, (**b**) electrical conductivity, and (**c**) electrical resistivity measured at 293 K of the as-deposited and heat-treated Cu/5Ag samples in radial (×), tangential (+), and longitudinal (○) directions.

The evolution of yield strength with temperature was studied with a tensile test, as shown in Figure 10. For this study, we chose to apply the following heat treatment on the material: 8 h at 330 °C. As expected, there was a gradual decrease in yield strength with the increase in temperature. At 100 °C, the yield strength was still above 500 MPa and reached approximatively 430 MPa at 200 °C.

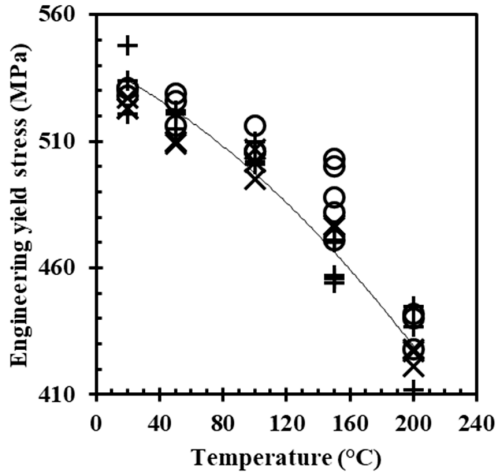

Figure 10. Evolution of engineering yield strength in radial (×), tangential (+), and longitudinal (○) directions with temperature for the Cu/5Ag CS-deposited material with an 8 h heat treatment at 330 °C.

3.2.2. Wires

The Vickers microhardness of a transverse section of wires was measured at different diameters (Figure 11).

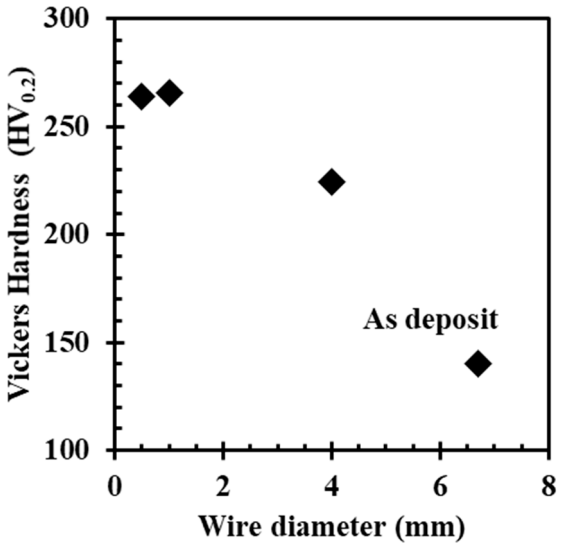

Figure 11. Vickers microhardness of the present samples. As-deposited value is from [8].

The values range from 140 HV (as-deposited sample in [8]) to 260 HV (Ø = 0.2 mm). For pure annealed Cu with a grain size ranging from 10 to 20 µm, the Vickers microhardness was about 45–50 HV. The Vickers microhardness of the deposit was about 140 HV, highlighting the effect of hardening due to the impact of particles and the presence of silver in the solid solution. The Vickers microhardness values increase when the diameter of the wire decreases, reflecting the refinement of the microstructure.

Typical stress–strain curves for the Cu/5Ag 0.8 mm wires at 293 K and 77 K are shown in Figure 12. During the tensile test, it was not possible to follow the strain with an extensometer due to the small diameter of wires and the testing itself being performed at 77 K. Strain was determined from crosshead displacement without any correction of machine rigidity. Therefore, it is not possible to discuss strain values and only UTS values can be studied.

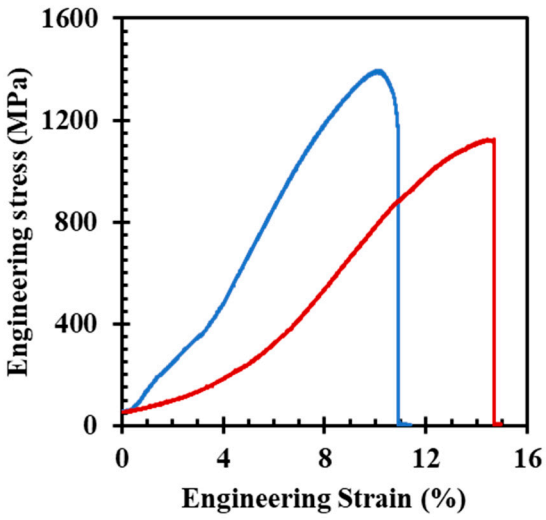

Figure 12. Stress–strain curves at 293 K (–) and 77 K (–) for the 0.8 mm diameter wire.

The UTS of wires of decreasing diameter (1–0.2 mm) was measured at 293 K and at 77 K (Figure 13a and Table 1). The UTS value was in the range of 855–1372 MPa at 293 K

and in the range of 1307–1660 MPa at 77 K. The UTS increases upon the decrease in wire diameter, reflecting the refinement of the microstructure. The higher values at 77 K could reflect the lower mobility of the dislocations at liquid nitrogen temperature. Some tested wires presented brittle fractures (Table 1), certainly due to localized defects (macroscopic dense Ag domains or porosity, as shown in Figures 3 and 4). As for bulk materials, heat treatment could be beneficial for ductility [9].

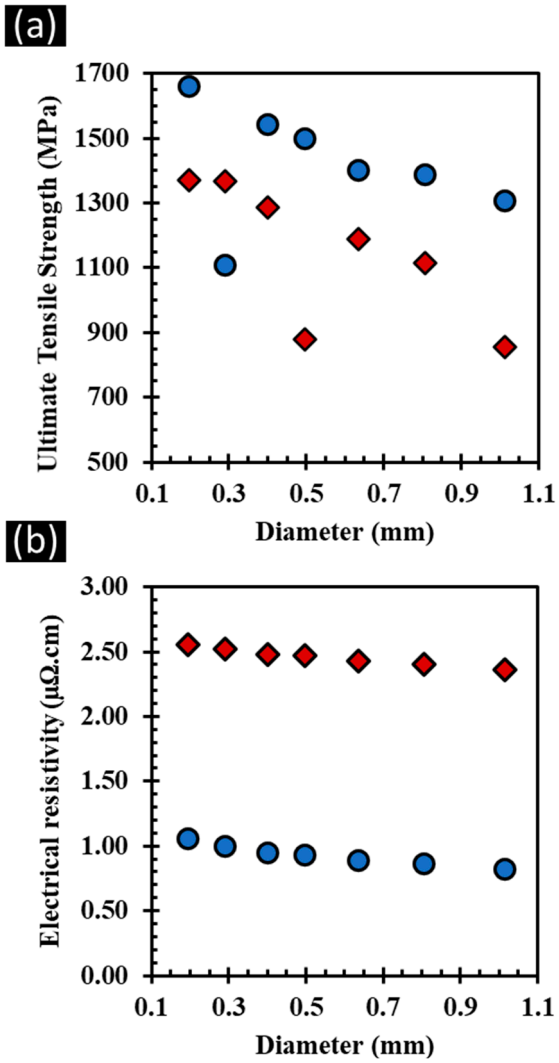

Figure 13. UTS vs. wire diameter (**a**) and electrical resistivity vs. wire diameter (**b**) at 293 K (◆) and 77 K (●) for present wires.

Table 1. Electrical resistivity and ultimate tensile strength (* indicates brittle fracture) at 293 K and 77 K for different wire diameters.

Wire Diameter (mm)	Electrical Resistivity (μΩ·cm)		Ultimate Tensile Strength (MPa)	
	293 K	77 K	293 K	77 K
1.0	2.37	0.82	855 *	1307
0.8	2.40	0.86	1115	1387
0.6	2.43	0.89	1187	1401
0.5	2.47	0.93	879 *	1499
0.4	2.48	0.95	1286	1541
0.3	2.52	1.00	1366	1108 *
0.2	2.56	1.05	1372	1660

The electrical resistivity (Figure 13b and Table 1) is in the range of 2.37–2.56 μΩ·cm at 293 K and in the range of 0.82–1.05 μΩ·cm at 77 K. The higher electrical resistivity of the finer wires is due to the increased density of grain boundaries, which act as scattering centers for conduction electrons. The lower values at 77 K can be explained by the negligible electron–phonon interactions at low temperature.

The UTS vs. electrical resistivity data were plotted at 77 K (Figure 14a) and at 293 K (Figure 14b). At 77 K, the present Cu/5Ag CS-alloyed wires showed a significantly higher UTS (1307–1660 MPa) than that reported for eutectic Cu/Ag-alloyed wires (940–1160 MPa) containing about four times more silver [4–6]. In those samples, the strengthening is mainly attributed to solid solution hardening and grain refinement. However, in the case of wires developed by CS, the high velocity of the deposited particles leads to high initial deformation rates and a specific dual microstructure that may explain the increased mechanical properties. This increase in the value of UTS is accompanied by a slight increase in the resistivity of the Cu/5Ag CS-alloyed wires (0.82–1.05 μΩ·cm) compared to the eutectic Cu/Ag-alloyed wires (0.7–0.8 μΩ·cm) [4–6]. The UTS values for the present wires were higher than those for the Cu/5Ag composite wires (963–1215 MPa) prepared by the SPS route [10]. However, the presence of solid solution makes CS wires (0.82–1.05 μΩ·cm) much more resistive than SPS Ag-Cu composites (0.42–0.7 μΩ·cm) whose copper matrix remains pure [11]. The trends thus described at 77 K are also observed at 293 K.

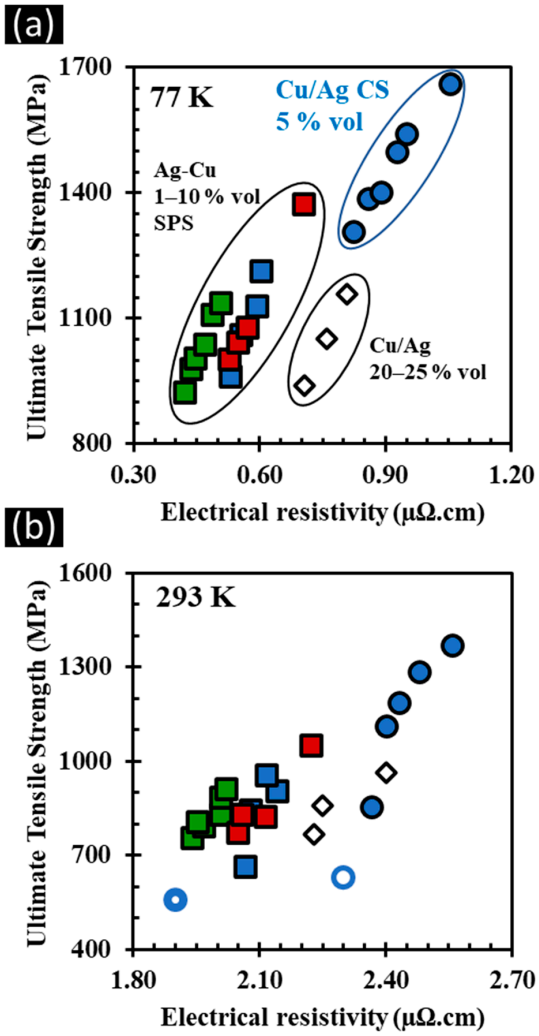

Figure 14. UTS vs. electrical resistivity at 77 K (**a**) and 293 K (**b**) for the present Cu/5Ag CS-alloyed wires (●) and bulk *CS* as-deposited (○) and heat-treated (⊙) SPS composite Ag-Cu (1, 5, and 10 vol. % Ag) wires (■, ■, ■) [10] and alloyed Cu/Ag (21–25 vol. % Ag) wires (◇) [4–6].

4. Conclusions

Cu/5Ag bulk cylinders prepared by CS under a helium atmosphere are now used for steady magnetic field production. They have totally replaced forged products that were much too limited both in mechanical and electrical properties. The typical properties obtained and adapted for DC production up to 45 T are 500 to 600 MPa for UTS at 293 K with a typical electrical conductivity of 49 MS/m (electrical resistivity = 2.03 μΩ·cm). These properties can be tuned thanks to heat-softening post treatments.

For steady-field production, the difference in yield strength values between the radial direction (about 500 MPa) and tangential and longitudinal directions (about 630 MPa) seems not to be critical, as the main Lorentz forces are along the tangential direction. This should be a point of attention for other applications. For the routine production of helices for magnetic steady- field production up to 37 T, we produce tubes with a minimum yield strength of 510 MPa at 293 K and a corresponding conductivity of 52 MS/m (1.92 μΩ·cm at 293 K). It is observed that the characteristic lifetime is higher than 5000 h. No accidental breaks have been observed in Cu/5Ag alloys during 9 years of field production using this technology. The leading indicator of lifetime seems to be the degradation with time of the epoxy joint between the consecutive turns of a given helix. Lorentz force calculations, including thermal load, show that the actual materials meet the requirements for our new hybrid magnet under commission which will be tested at 43 T in 2024 [1].

For non-destructive high magnetic pulsed-field applications, Cu/5Ag-alloyed wires were prepared by the room-temperature wire-drawing of cylinders, consolidated by the CS technique, without breaking. It is shown that theses wires offer a combination of very high strength (1660 MPa at 77 K) and low electrical resistivity (1.05 μΩ·cm at 77 K), and compare favorably with Cu/Ag-alloyed wires produced by classical metallurgy containing about four times more silver. This improvement may be attributed to the specific dual microstructure induced by the high velocity of the deposited particles and associated high initial deformation rates. Moreover, using a small proportion of Ag (5% vol. Ag) avoids an excessive increase in electrical resistivity. The CS manufacturing route therefore appears suitable for the production of larger Cu/5Ag-alloyed precursors for wire drawing.

Author Contributions: Investigation, S.T., H.I., C.V., O.J., N.F., A.J., C.T. and F.L.-D.; Resources, S.T., C.V., O.J. and N.F.; Supervision, F.D, L.T. and F.L.-D.; Writing—original draft, S.T., H.I., C.V., O.J. and F.D; Writing—review & editing, S.T., H.I., C.V., O.J., N.F., F.D., A.J., C.T., L.T. and F.L.-D. All authors have read and agreed to the published version of the manuscript.

Funding: This work was financially supported by the Agence Nationale de la Recherche (ANR-20-CEO8-0027). This work was supported by the French government programme "Investissements d'Avenir" (LABEX INTERACTIFS, reference ANR-11-LABX-0017-01, and EUR INTREE, reference ANR-18-EURE-0010). This work has been partially supported by "Région Nouvelle Aquitaine" (CPER) and 617 "Fonds Européen de Développement Régional (FEDER)" through the use of the Focused Ion Beam (FIB) (reference P-2016-BAFE) and the use of the microscope FEI-TALOS (P-2020-BAFE-5).

Institutional Review Board Statement: Not applicable.

Informed Consent Statement: Not applicable.

Data Availability Statement: Data will be made available on request.

Acknowledgments: The authors thank T. Schiavo, L. Bendichou for the preparation of the billets.

Conflicts of Interest: The authors declare no conflicts of interest.

References

1. Pugnat, P.; Barbier, R.; Berriaud, C.; Berthier, R.; Boujet, T.; Graffin, P.; Grandclement, C.; Hervieu, B.; Jousset, J.; Juster, F.P.; et al. 43 + T Grenoble Hybrid Magnet: From Final Assembly to Commissioning of the Superconducting Outsert. *IEEE Trans. Appl. Supercond.* **2022**, *32*, 4300607. [CrossRef]
2. Beard, J.; Billette, J.; Ferreira, N.; Frings, P.; Lagarrigue, J.-M.; Lecouturier, F.; Nicolin, J.-P. Design and Tests of the 100-T Triple Coil at LNCMI. *IEEE Trans. Appl. Supercond.* **2017**, *28*, 4300305. [CrossRef]

3. Sakai, Y.; Inoue, K.; Asano, T.; Wada, H.; Maeda, H. Development of high-strength, high-conductivity Cu–Ag alloys for high-field pulsed magnet use. *Appl. Phys. Lett.* **1991**, *59*, 2965–2967. [CrossRef]
4. Han, K.; Baca, A.; Coe, H.; Embury, J.; Kihara, K.; Lesch, B.; Li, L.; Schillig, J.; Sims, J.; Van Sciver, S.; et al. Material issues in the 100 T non-destructive magnet. *IEEE Trans. Appl. Supercond.* **2000**, *10*, 1277–1280. [CrossRef]
5. Han, K.; Embury, J.; Sims, J.; Campbell, L.; Schneider-Muntau, H.-J.; Pantsyrnyi, V.; Shikov, A.; Nikulin, A.; Vorobieva, A. The fabrication, properties and microstructure of Cu–Ag and Cu–Nb composite conductors. *Mater. Sci. Eng. A* **1999**, *267*, 99–114. [CrossRef]
6. Zuo, X.; Han, K.; Zhao, C.; Niu, R.; Wang, E. Microstructure and properties of nanostructured Cu28 wt%Ag microcomposite deformed after solidifying under a high magnetic field. *Mater. Sci. Eng. A* **2014**, *619*, 319–327. [CrossRef]
7. Coddet, P.; Verdy, C.; Coddet, C.; Debray, F. Effect of cold work, second phase precipitation and heat treatments on the mechanical properties of copper–silver alloys manufactured by cold spray. *Mater. Sci. Eng. A* **2015**, *637*, 40–47. [CrossRef]
8. Coddet, P.; Verdy, C.; Coddet, C.; Debray, F. On the mechanical and electrical properties of copper-silver and copper-silver-zirconium alloys deposits manufactured by cold spray. *Mater. Sci. Eng. A* **2016**, *662*, 72–79. [CrossRef]
9. Jay, O.; Verdy, C.; Trophime, C.; Danlos, Y.; Debray, F. Cold Spray Manufacturing for Structural Materials for High Field Magnet Production. *Mater. Sci. Forum* **2018**, *941*, 1540–1545. [CrossRef]
10. Tardieu, S.; Mesguich, D.; Lonjon, A.; Lecouturier, F.; Ferreira, N.; Chevallier, G.; Proietti, A.; Estournès, C.; Laurent, C. Nanostructured 1% silver-copper composite wires with a high tensile strength and a high electrical conductivity. *Mater. Sci. Eng. A* **2019**, *761*, 138048. [CrossRef]
11. Tardieu, S.; Mesguich, D.; Lonjon, A.; Lecouturier-Dupouy, F.; Ferreira, N.; Chevallier, G.; Proietti, A.; Estournès, C.; Laurent, C. Influence of alloying on the tensile strength and electrical resistivity of silver nanowire: Copper composites macroscopic wires. *J. Mater. Sci.* **2020**, *56*, 4884–4895. [CrossRef]
12. Tardieu, S.; Mesguich, D.; Lonjon, A.; Lecouturier-Dupouy, F.; Ferreira, N.; Chevallier, G.; Proietti, A.; Estournès, C.; Laurent, C. Influence of bimodal copper grain size distribution on electrical resistivity and tensile strength of silver–copper composite wires. *Mater. Today Commun.* **2023**, *37*, 107403. [CrossRef]
13. Schmidt, T.; Gärtner, F.; Assadi, H.; Kreye, H. Development of a generalized parameter window for cold spray deposition. *Acta Mater.* **2006**, *54*, 729–742. [CrossRef]
14. Assadi, H.; Kreye, H.; Gärtner, F.; Klassen, T. Cold spraying–A materials perspective. *Acta Mater.* **2016**, *116*, 382–407. [CrossRef]
15. Hassani-Gangaraj, M.; Veysset, D.; Nelson, K.A.; Schuh, C.A. In-situ observations of single micro-particle impact bonding. *Scr. Mater.* **2018**, *145*, 9–13. [CrossRef]
16. Hassani-Gangaraj, M.; Veysset, D.; Champagne, V.K.; Nelson, K.A.; Schuh, C.A. Adiabatic shear instability is not necessary for adhesion in cold spray. *Acta Mater.* **2018**, *158*, 430–439. [CrossRef]
17. Assadi, H.; Gärtner, F.; Stoltenhoff, T.; Kreye, H. Bonding mechanism in cold gas spraying. *Acta Mater.* **2003**, *51*, 4379–4394. [CrossRef]
18. Grujicic, M.; Zhao, C.; DeRosset, W.; Helfritch, D. Adiabatic shear instability based mechanism for particles/substrate bonding in the cold-gas dynamic-spray process. *Mater. Des.* **2004**, *25*, 681–688. [CrossRef]
19. Luo, X.-T.; Li, C.-X.; Shang, F.-L.; Yang, G.-J.; Wang, Y.-Y.; Li, C.-J. High velocity impact induced microstructure evolution during deposition of cold spray coatings: A review. *Surf. Coat. Technol.* **2014**, *254*, 11–20. [CrossRef]
20. Chaudhuri, A.; Raghupathy, Y.; Srinivasan, D.; Suwas, S.; Srivastava, C. Microstructural evolution of cold-sprayed Inconel 625 superalloy coatings on low alloy steel substrate. *Acta Mater.* **2017**, *129*, 11–25. [CrossRef]
21. Liu, T.; Leazer, J.D.; Brewer, L.N. Particle deformation and microstructure evolution during cold spray of individual Al-Cu alloy powder particles. *Acta Mater.* **2019**, *168*, 13–23. [CrossRef]
22. Rokni, M.; Widener, C.; Crawford, G. Microstructural evolution of 7075 Al gas atomized powder and high-pressure cold sprayed deposition. *Surf. Coat. Technol.* **2014**, *251*, 254–263. [CrossRef]
23. Huang, R.; Sone, M.; Ma, W.; Fukanuma, H. The effects of heat treatment on the mechanical properties of cold-sprayed coatings. *Surf. Coat. Technol.* **2015**, *261*, 278–288. [CrossRef]
24. Qiu, X.; Wang, J.-Q.; Tariq, N.U.H.; Gyansah, L.; Zhang, J.-X.; Xiong, T.-Y. Effect of Heat Treatment on Microstructure and Mechanical Properties of A380 Aluminum Alloy Deposited by Cold Spray. *J. Therm. Spray Technol.* **2017**, *26*, 1898–1907. [CrossRef]